Electronic Supplementary Information

Self-operating transpiration-driven electrokinetic power generator with an artificial hydrological cycle.

Jaehyeong Bae[a†], Tae Gwang Yun[a†], Bong Lim Suh[b], Jihan Kim[b], Il-Doo Kim[a*]

[a]Department of Materials Science and Engineering, Korea Advanced Institute of Science and Technology (KAIST), 291 Daehak-ro, Yuseong-gu, Daejeon, 34141, Republic of Korea.

[b]Department of Chemical and Biomolecular Engineering, Korea Advanced Institute of Science and Technology (KAIST), 291 Daehak-ro, Yuseong-gu, Daejeon, 34141, Republic of Korea.

[†]These authors contributed equally to this work.

[*]Correspondence to: Il-Doo Kim; E-mail: idkim@kaist.ac.kr

Study of resistance elements in the STEPG for analysis of V_{OC} and I_{SC}.

The resistance elements in the STEPG device can be analyzed as shown in Fig. S2a. These elements include R_w (carbon coated on the wet region), R_{ii} (the innermost carbon layer attached to cotton at the wet/dry interface), R_{ie} (excess exterior carbon layer at the wet/dry interface), and R_d (carbon coated on the dry region). V_{EDL} and I_{PST} denote the potential difference due to the electrical double layer and the pseudostreaming current, respectively.

The voltage at the terminal is V_{EDL} minus the voltage loss over the series resistances (R_{ii}, R_w, and R_d).

$$V = V_{EDL} - I_{PST}R_{ii} - I(R_w + R_d) \tag{1}$$

The current at the terminal is I_{PST} minus the shunt current (I_{sh}) leaking through the shunt resistance (R_{ie}).

$$I = I_{PST} - I_{sh} \tag{2}$$

The shunt current is the potential applied to the shunt resistance divided by the shunt resistance.

$$I_{sh} = \frac{V_{EDL} - I_{PST}R_{ii}}{R_{ie}} \tag{3}$$

Combining equation (2) and equation (3),

$$I = I_{PST} - \frac{V_{EDL} - I_{PST}R_{ii}}{R_{ie}} \tag{4}$$

Rearranging equation (4),

$$I_{PST} = \frac{V_{EDL} + IR_{ie}}{R_{ii} + R_{ie}} \tag{5}$$

Combining equation (1) and equation (5),

$$V = V_{EDL} - \frac{V_{EDL} + IR_{ie}}{R_{ii} + R_{ie}}R_{ii} - I(R_w + R_d) \tag{6}$$

By the definition of the open-circuit voltage, the current at the terminal is zero. Therefore, equation (6) becomes

$$V_{OC} = V_{EDL} - \frac{V_{EDL}R_{ii}}{R_{ii} + R_{ie}} = V_{EDL}\left(1 - \frac{R_{ii}}{R_{ii} + R_{ie}}\right) \tag{7}$$

From equation (7), we can see that a reduction of the internal resistance increases the fraction in parentheses, which results in a decrease of V_{OC} (Fig. 3a).

Rearranging equation (5),

$$V_{EDL} = I_{PST}(R_{ii} + R_{ie}) - IR_{ie} \tag{8}$$

Combining equation (1) and equation (8),

$$I = \frac{I_{PST}R_{ie} - V}{R_{ie} + R_w + R_d} \tag{9}$$

By the definition of the short-circuit current, the voltage at the terminal is zero. Therefore, equation (9) becomes

$$I_{SC} = \frac{I_{PST}R_{ie}}{R_{ie} + R_w + R_d} = \frac{I_{PST}}{1 + \frac{R_w + R_d}{R_{ie}}} \tag{10}$$

The resistance effect on I_{SC} is hard to see from equation (10).
Let us assume that V_{EDL} and I_{PST} are constant, as the origin of V_{EDL} and I_{PST} is not related to the amount of Ketjen black.
Combining equation (4) and equation (10),

$$I_{SC} = \frac{V_{EDL}}{R_{ii} + (R_w + R_d)\left(1 + \frac{R_{ii}}{R_{ie}}\right)} \tag{11}$$

Dropping $CaCl_2$ solution onto the STEPG decreases R_{ii}, R_{ie}, and R_w (Table S1). R_w and R_d are connected in series with a wet/dry interface. If the STEPG generates a current, then the voltage would decrease over R_w and R_d. From equation (11), we can confirm that the reduction of R_{ii}, R_{ie}, and R_w due to the addition of salt decreases the denominator, which results in an increase of I_{SC}.

Comparison of V_{EDL} originating from the STEPG and TEPG and the V_{EDL} generated by dropping $CaCl_2$ solution on the negative electrode and DI water on the positive electrode.

From Fig. 2c, the measured V_{OC} generated by dropping $CaCl_2$ solution and DI water on the negative and positive electrodes, respectively, seems to not match the V_{OC} of the STEPG ($CaCl_2$) minus the V_{OC} of the TEPG (water). As V_{OC} is influenced by the various internal resistances, comparing the V_{EDL} values is more appropriate. Based on equation (7), we calculated the V_{EDL} of the STEPG ($CaCl_2$) and TEPG (water) from the measured V_{OC} and reference resistance values in Table 1, S1a. For the STEPG fully wetted by $CaCl_2$ solution at the negative electrode and water at the positive electrode, the resistance elements can be analyzed as shown in Fig. S2b. Following a similar analysis as above, we can obtain the V_{OC} of the fully wetted STEPG.

$$V_{OC} = \frac{(V_{EDL,CaCl2} - V_{EDL,water})R_{i,water}}{R_{i,CaCl2} + R_{i,water}} \tag{12}$$

where $R_{w,CaCl2}$: carbon wetted by $CaCl_2$, $R_{i,CaCl2}$: innermost carbon layer at the wet/dry interface that contains mostly $CaCl_2$, $R_{i,water}$: exterior carbon layer at the wet/dry interface that contains mostly water, and $R_{w,water}$: carbon wetted by water. $V_{EDL,CaCl2}$-$V_{EDL,water}$ denotes the potential difference due to the electrical double layer formed by $CaCl_2$ solution and water. Using equation (12), we calculated $V_{EDL,CaCl2}$-$V_{EDL,water}$ from the measured V_{OC} and reference resistance values in Table 1, S1a. The value of $V_{EDL,CaCl2}$-$V_{EDL,water}$ fairly matches the V_{EDL} of the STEPG ($CaCl_2$) minus that of the TEPG (water), which confirms that the measured V_{OC} originates from the potential difference between the electrical double layers formed on the carbon wetted by the $CaCl_2$ solution and DI water.

Comparison of I_{PST} originating from the STEPG and TEPG and the I_{SC} generated by dropping $CaCl_2$ solution on the negative electrode and DI water on the positive electrode.

From Fig. S4, the measured I_{SC} generated by dropping $CaCl_2$ solution and DI water on the negative and positive electrodes, respectively, seems to not match the I_{SC} of the STEPG ($CaCl_2$) minus the I_{SC} of the TEPG (water). As I_{SC} is influenced by the various internal resistances, comparing the I_{PST} values is more appropriate. Based on equation (10), we calculated the I_{PST} of the STEPG ($CaCl_2$) and TEPG (water) from the measured I_{SC} and reference resistance values in Table S1. For the STEPG fully wetted by $CaCl_2$ solution at the negative electrode and water at the positive electrode, the resistance elements can be analyzed as shown in Fig. S2b. Following a similar analysis as above, we can obtain the I_{SC} of the fully wetted STEPG.

$$I_{SC} = \frac{I_{PST,CaCl2} - I_{PST,water}}{1 + \dfrac{R_{w,CaCl2} + R_{w,water}}{R_{i,water}}} \tag{13}$$

where $I_{PST,CaCl2}$ - $I_{PST,water}$ represents the pseudostreaming current difference due to $CaCl_2$ solution and water. Using equation (13), we calculated $I_{PST,CaCl2}$ - $I_{PST,water}$ from the measured

I_{SC} and reference resistance values in Table S1. The value of $I_{PST,CaCl2}$ - $I_{PST,water}$ is larger than the I_{SC} of the TEPG (water), showing that the pseudostreaming current from the $CaCl_2$ solution to water is larger than that from the wetted area to dry area. This phenomenon partially contributed to the higher charge density due to the additional Ca^{2+} ions on the carbon surface and partially contributed to the conductivity of the solution. The value of $I_{PST,CaCl2}$ - $I_{PST,water}$ is far smaller than the I_{PST} of the STEPG ($CaCl_2$), which shows that the flow rate of the stream is largely decreased by the reduced water content gradient.

Electron transfer in carbon layer.

Since the carbon nanoparticles are coated on cotton fabric by dip coating, some of the particles have good physical contacts but the other particles have close and mediocre contacts. In some portion, therefore, water exist in between the carbon particles. This can be proved by monitoring resistance change of STEPG (Table S1). Ketjen black-coated cotton fabric got higher resistance after wetting, because water is poorer conductor than Ketjen black. This result indicates that water exist in between some of the carbon particles. Addition of solution inevitably hinders electron transfer; however, electrolytes ($CaCl_2$) facilitate the electron transfer, which is one of the huge advantage of using electrolyte solution as a fuel for TEPG.

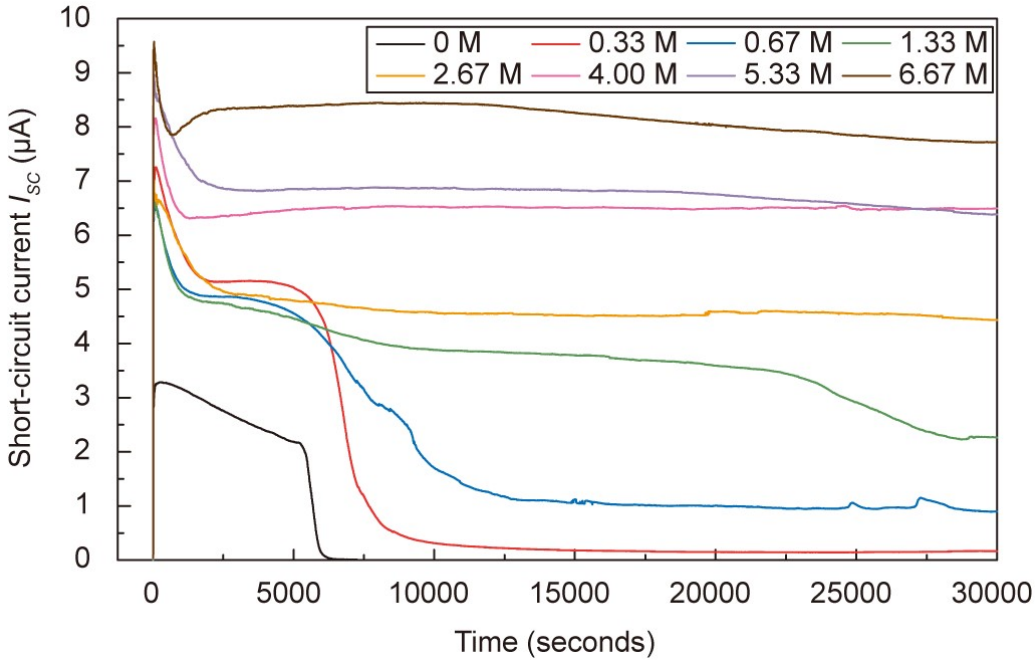

Fig. S1 Measured I_{SC} profiles generated by dropping various concentrations of $CaCl_2$ solution on the STEPG (120 kΩ) at 26 ℃ and 40% RH.

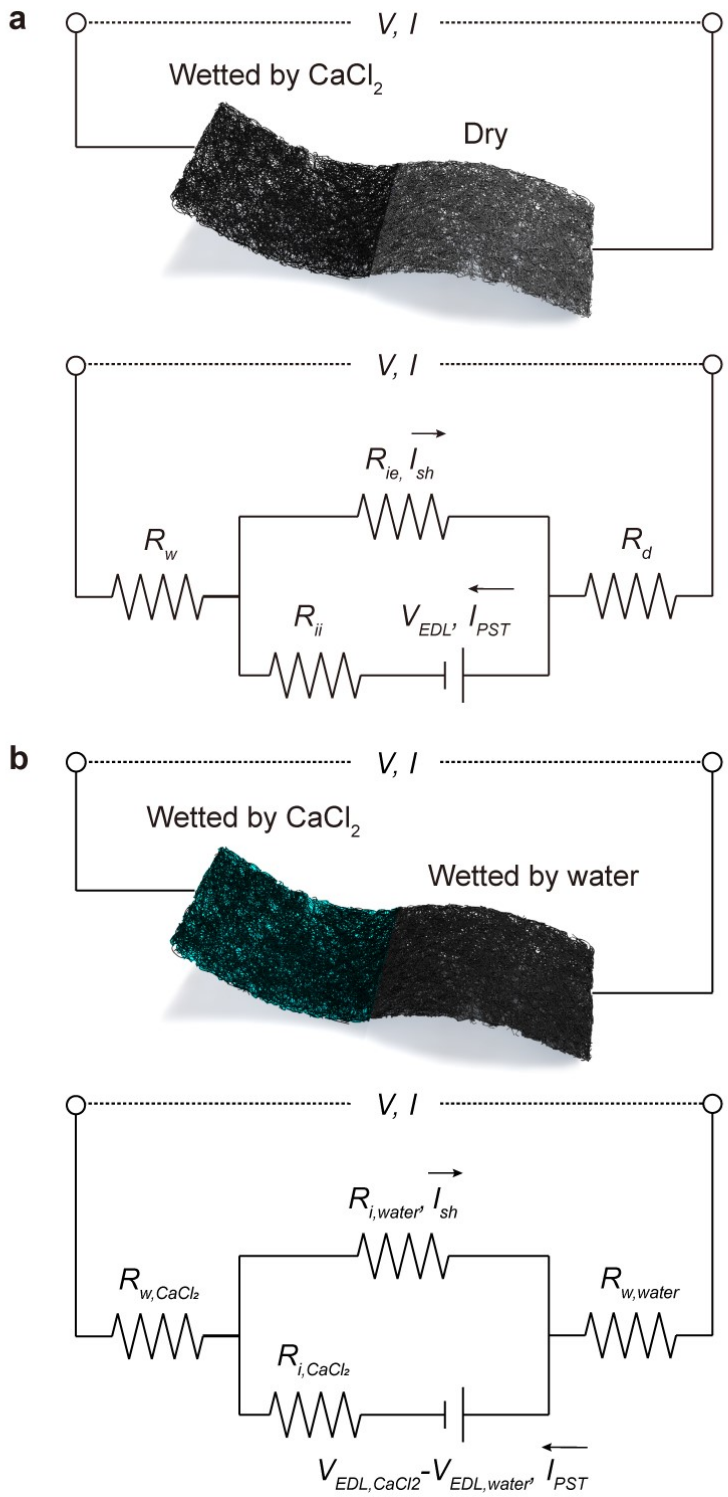

Fig. S2 (a) Schematic illustration of the working STEPG and the corresponding electric circuit. **(b)** Schematic illustration of the working STEPG wetted by $CaCl_2$ solution and water at each electrode and the corresponding electric circuit.

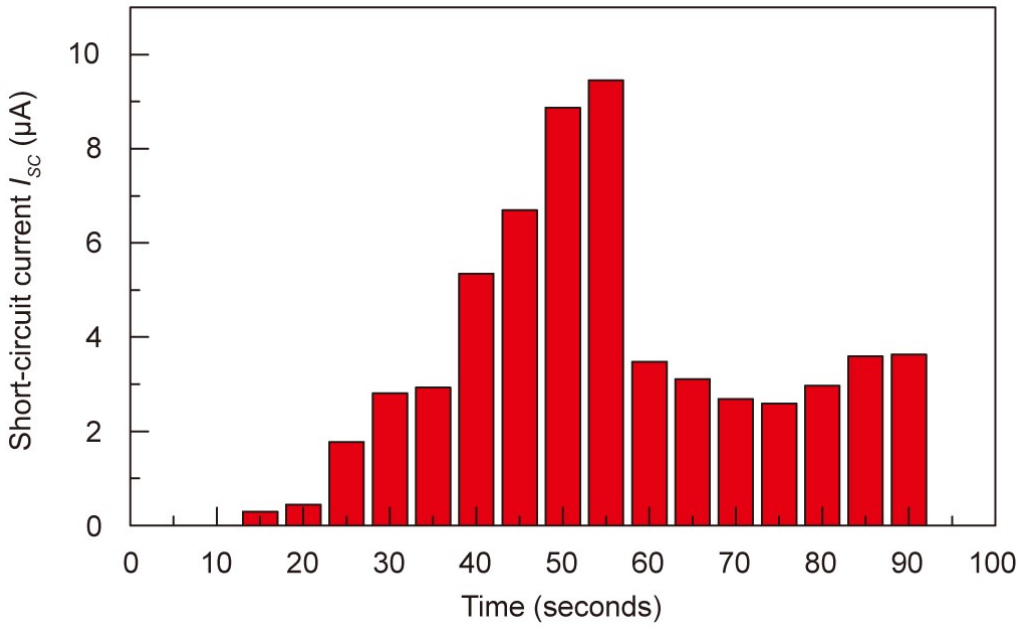

Fig. S3 Measured I_{SC} of the STEPG (120 kΩ) at various RH conditions and 22 ℃.

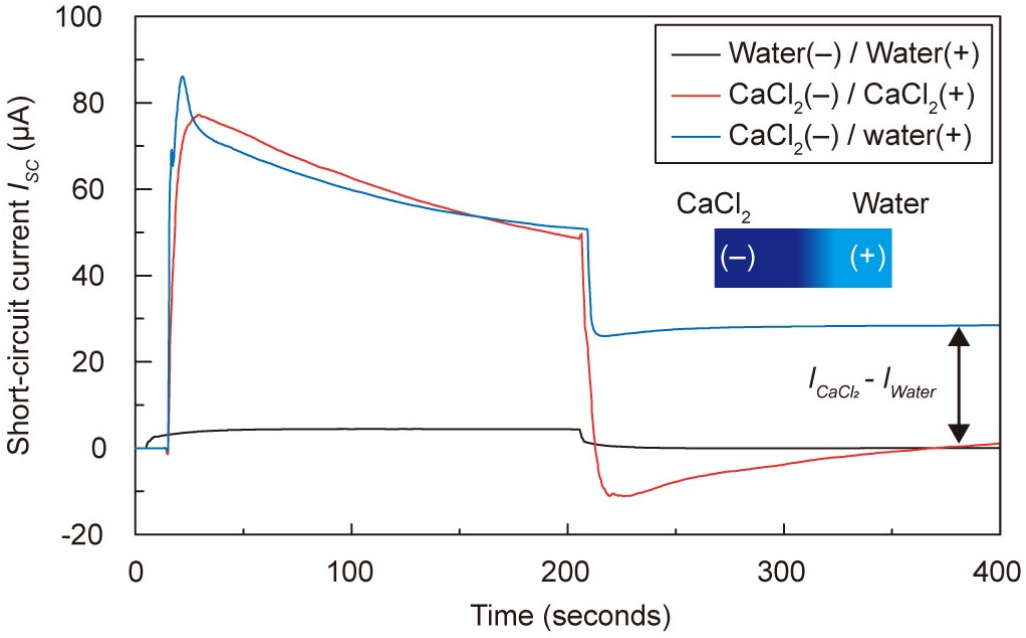

Fig. S4 Measured I_{SC} of the STEPG generated by dropping various combinations of DI water and saturated $CaCl_2$ solution on the (-) and (+) electrodes.

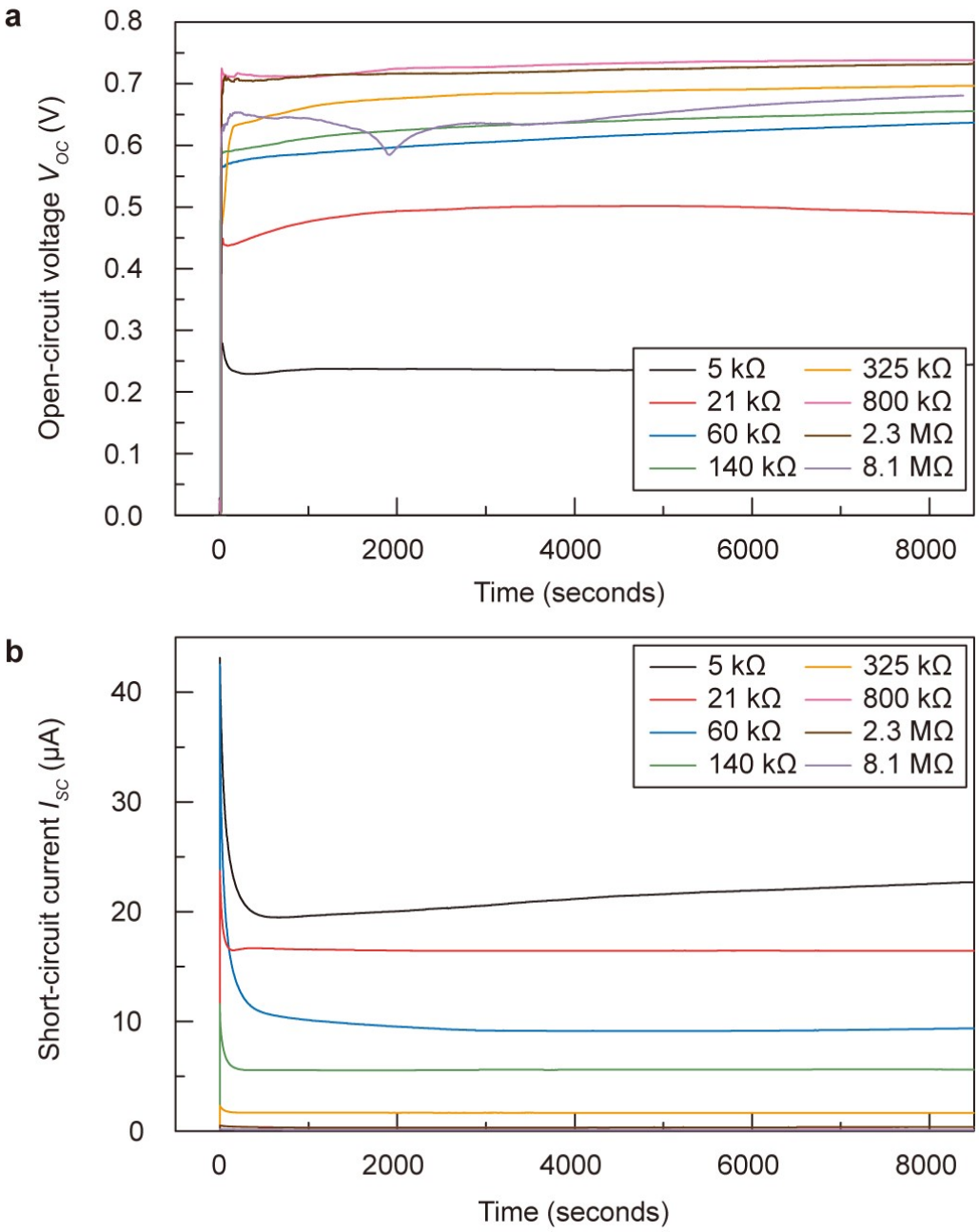

Fig. S5 (a) and **(b)** Measured V_{OC} and I_{SC} profiles, respectively, generated by dropping 0.25 mL of saturated $CaCl_2$ solution on various resistance STEPGs.

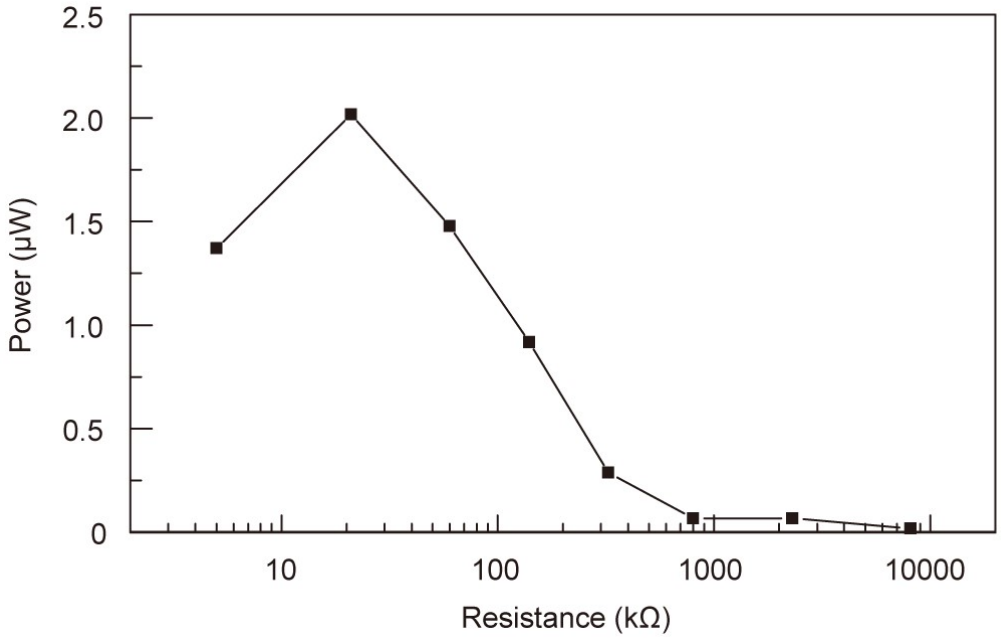

Fig. S6 Measured power of STEPGs with various resistances at 26 ℃ and 37% RH.

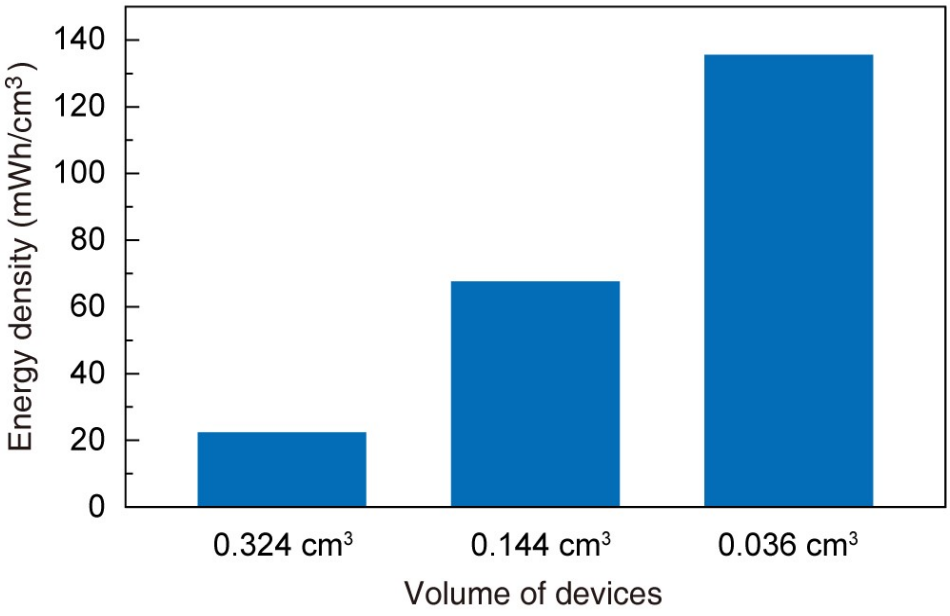

Fig. S7 Measured energy density of STEPGs with various dimension of the devices at 26 ℃ and 37% RH. The resistance of the device was fixed to 21 kΩ for all devices.

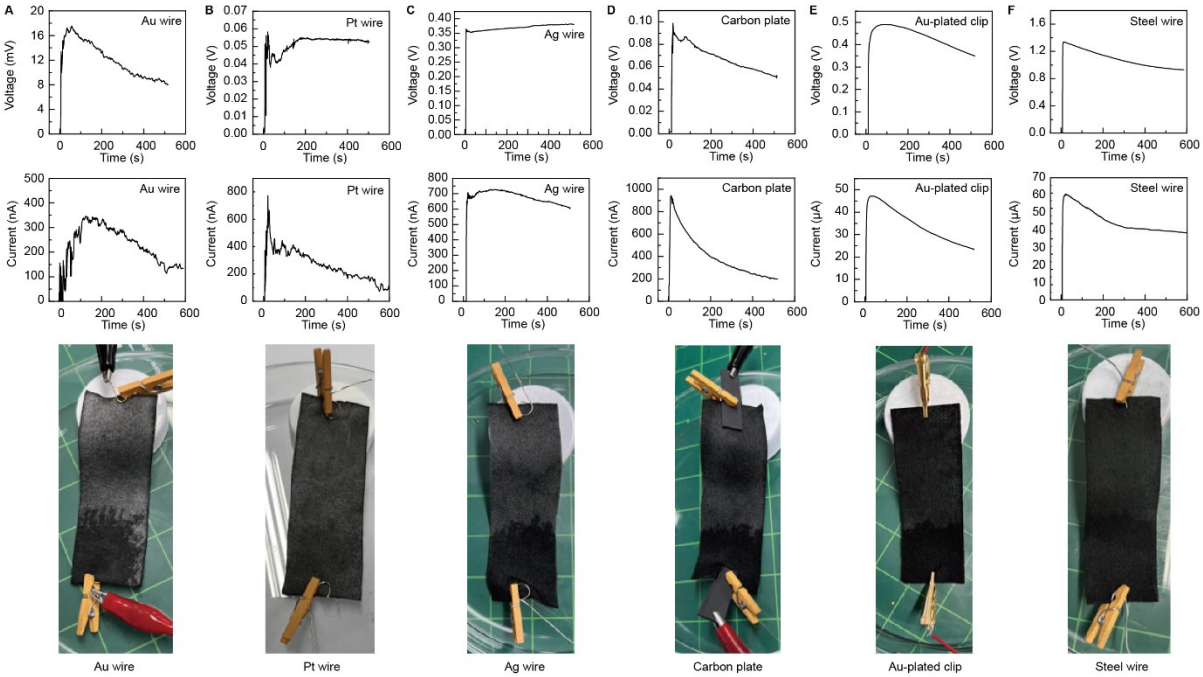

Fig. S8 Voltage and current measured by STEPG (100 kΩ) with Au, Pt, Ag, steel wires, carbon plates, and Au-plated clip, and their photographic pictures.

Table S1 a, Resistance of Ketjen black-coated cotton fabric in the conditions of dry, wetted by $CaCl_2$ solution, and wetted by water. **b**, Measured I_{SC} and calculated I_{PST} or $I_{PST,CaCl2}$-$I_{PST,water}$ generated by dropping DI water or saturated $CaCl_2$ solution on the (-) electrode or dropping saturated $CaCl_2$ solution and water on the (-) and (+) electrodes, respectively.

a

Ketjen black-coated cotton fabric	Resistance
Dry	7.4 kΩ
Wetted by $CaCl_2$ solution	2.4 kΩ
Wetted by water	30.15 kΩ

b

Ketjen black-coated cotton fabric (7.4 kΩ)	I_{SC}	I_{PST} or $I_{PST,CaCl2} - I_{PST,water}$
(1) $CaCl_2$ (–) / dry (+)	53.88 μA	273.91 μA
(2) Water (–) / dry (+)	4.88 μA	10.96 μA
(3) $CaCl_2$ (–) / water (+)	30.02 μA	62.44 μA

Table S2 Summary of water-based electricity generation devices. The energy performance is compared based on a single unit.

No.	Material / Method	Voltage (V)	Current (μA)	Power (μW)	Ref.
1	Graphene / Water stream		0.5		1
2	Boron nitride nanotube / Water osmosis	0.05	0.0015	0.000019	2
3	Glass and PDMS / Water stream	0.16	0.0018	0.00002	3
4	MoS2 / Water stream	0.1	0.01	0.00025	4
5	MWCNT fiber / Water stream	0.18	24	1.08	5
6	Carbon / Water evaporation	1	0.15	0.053	6
7	Graphene oxide / Moisture	0.7	0.3	0.212	7
8	Reduced graphene oxide / Moisture	0.45	0.034	0.08	8
9	Graphene oxide / Water diffusion	1.5	0.2	0.075	9
10	Carbon sponge / Water evaporation	10 (pulse)	0.02	0.05	10
11	Porous polydopamine / Moisture	0.52	1.86	0.148	11
12	Graphene oxide composite / Moisture	0.6	0.12	0.007	12
13	Mxene/Kevlar Water osmosis	~0.12	4.8	0.123	13
This work	Carbon nanoparticle / Water stream	0.74	22.5	2.02	

Reference

1 W. Guo, C. Cheng, Y. Wu, Y. Jiang, J. Gao, D. Li and L. Jiang, *Adv. Mater.*, 2013, **25**, 6064–6068.

2 A. Siria, P. Poncharal, A. L. Biance, R. Fulcrand, X. Blase, S. T. Purcell and L. Bocquet, *Nature*, 2013, **494**, 455–458.

3 R. Zhang, S. Wang, M. H. Yeh, C. Pan, L. Lin, R. Yu, Y. Zhang, L. Zheng, Z. Jiao and Z. L. Wang, *Adv. Mater.*, 2015, **27**, 6482–6487.

4 J. Feng, M. Graf, K. Liu, D. Ovchinnikov, D. Dumcenco, M. Heiranian, V. Nandigana, N. R. Aluru, A. Kis and A. Radenovic, *Nature*, 2016, **536**, 197–200.

5 Y. Xu, P. Chen, J. Zhang, S. Xie, F. Wan, J. Deng, X. Cheng, Y. Hu, M. Liao, B. Wang, X. Sun and H. Peng, *Angew. Chemie - Int. Ed.*, 2017, **56**, 12940–12945.

6 G. Xue, Y. Xu, T. Ding, J. Li, J. Yin, W. Fei, Y. Cao, J. Yu, L. Yuan, L. Gong, J. Chen, S. Deng, J. Zhou and W. Guo, *Nat. Nanotechnol.*, 2017, **12**, 317–321.

7 Y. Liang, F. Zhao, Z. Cheng, Y. Deng, Y. Xiao, H. Cheng, P. Zhang, Y. Huang, H. Shao and L. Qu, *Energy Environ. Sci.*, 2018, **11**, 1730–1735.

8 H. Cheng, Y. Huang, F. Zhao, C. Yang, P. Zhang, L. Jiang, G. Shi and L. Qu, *Energy Environ. Sci.*, 2018, **11**, 2839–2845.

9 Y. Huang, H. Cheng, C. Yang, P. Zhang, Q. Liao, H. Yao, G. Shi and L. Qu, *Nat. Commun., 2018,* **9**, 4166.

10 L. Zhu, M. Gao, C. K. N. Peh, X. Wang and G. W. Ho, *Adv. Energy Mater.*, 2018, **8**, 1–8.

11 L.-H. Li, Z. Chen, M. Hao, S. Wang, F. Sun, Z. Zhao and T. Zhang, *Nano Lett.*, 2019, **19**, 5544-5552.

12 Y. Huang, H. Cheng, C. Yang, H. Yao, C. Li and L. Qu, *Energy Environ. Sci.*, 2019, **12**, 1848–1856.

13 Z. Zhang, S. Yang, P. Zhang, J. Zhang, G. Chen and X. Feng, *Nat. Commun.*, 2019, **10**, 2920.